Lipid packing defects and membrane charge control RAB GTPase recruitment

Guillaume Kulakowski, Hugo Bousquet, Jean-Baptiste Manneville, Patricia Bassereau, Bruno Goud, Lena K Oesterlin

Received: 13 October 2017 | Revised: 15 March 2018 | Accepted: 16 March 2018 | Uncorrected manuscript published: 23 March 2018 | Published on: 6 April 2018

DOI: 10.1111/tra.12568

WILEY Traffic

ORIGINAL ARTICLE

Lipid packing defects and membrane charge control RAB GTPase recruitment

Guillaume Kulakowski[1] | Hugo Bousquet[1] | Jean-Baptiste Manneville[1] | Patricia Bassereau[2] | Bruno Goud[1] | Lena K. Oesterlin[1]

[1]Institut Curie, Paris Sciences et Lettres Research University, Sorbonne Université, CNRS UMR144, Paris, France

[2]Laboratoire Physico Chimie, Institut Curie, Paris Sciences et Lettres Research University, Sorbonne Université, CNRS UMR168, Paris, France

Correspondence
Lena K. Oesterlin, Institut Curie, Paris Sciences et Lettres Research University, CNRS, UMR144, 26 rue d'Ulm, F-75005 Paris, France.
Email: lena.oesterlin@curie.fr

Funding information
FP7 People: Marie-Curie Actions, Marie Curie Intra European Fellowship, Grant/Award Number: PIEF-GA-2012-326649; FP7 Ideas: European Research Council, ERC advanced grant, Grant/Award Number: 339847 'MYODYN'

Specific intracellular localization of RAB GTPases has been reported to be dependent on protein factors, but the contribution of the membrane physicochemical properties to this process has been poorly described. Here, we show that three RAB proteins (RAB1/RAB5/RAB6) preferentially bind *in vitro* to disordered and curved membranes, and that this feature is uniquely dependent on their prenyl group. Our results imply that the addition of a prenyl group confers to RAB proteins, and most probably also to other prenylated proteins, the ability to sense lipid packing defects induced by unsaturated conical-shaped lipids and curvature. Consistently, RAB recruitment increases with the amount of lipid packing defects, further indicating that these defects drive RAB membrane targeting. Membrane binding of RAB35 is also modulated by lipid packing defects but primarily dependent on negatively charged lipids. Our results suggest that a balance between hydrophobic insertion of the prenyl group into lipid packing defects and electrostatic interactions of the RAB C-terminal region with charged membranes tunes the specific intracellular localization of RAB proteins.

KEYWORDS

curvature sensing, geranylgeranyl, lipid packing defects, membrane order, prenylation

1 | INTRODUCTION

RAB proteins are small GTPases of the RAS superfamily that are involved in many steps of transport inside the cell. There are over 60 RAB proteins in humans and they all localize to distinct membrane compartments. RAB proteins which oscillate between an active form (GTP-bound) and an inactive form (GDP-bound) can bind to membranes with the help of their prenyl group (geranylgeranyl group), a posttranslational lipid modification at their C-terminal extremity. The RAB escort protein (REP), known to be involved in RAB prenylation, and the GDP dissociation inhibitor (GDI), known to bind to soluble RABs, are known to play key roles in both the delivery and the recycling of RAB proteins to and from membranes[1,2] but cannot account for their specific intracellular localization. Until now, multiple studies have suggested that RAB-specific membrane targeting could be mediated by protein factors such as guanine nucleotide exchange factors (GEF), originally known to activate RABs by nucleotide exchange,[3] and GDI displacement factors, thought to influence the release of prenylated RAB proteins from GDI.[4,5] Extensive sequence analysis, domain swapping and mutagenesis studies of different RAB proteins have shown that specific domains are involved in RAB targeting to membranes. Pereira-Leal and Seabra[6] identified five RAB family regions that distinguish RAB proteins from the other members of the RAS superfamily and four subfamily regions that stand to differentiate each RAB subfamily. Different combinations of mutations of these domains led to mislocalization of the RAB proteins, suggesting that membrane specificity is also determined by specific RAB sequences.[7] The hypervariable region of RAB35 has also been shown to be determinant for proper membrane targeting.[8]

While protein–protein interaction has been widely studied to explain RAB-specific membrane targeting, very little is known about the influence of the membrane itself. Diverging from the initial fluid mosaic model,[9] it is now known that membranes are crowded and heterogeneous environments with lipids and proteins diffusing

laterally allowing the formation of regions which vary in thickness and composition.[10] Because of specific lipid metabolism and selective transport, cellular membranes have heterogeneous lipid compositions and can also be characterized by asymmetrical lipid compositions between the two leaflets.[11] Similarly to RAB proteins, some lipids localize to specific compartments and thereby also define organelle identity. Because of their diversity in lipid composition, intracellular membranes exhibit different physicochemical properties such as charge, lipid packing defects and membrane curvature.[12–14] The negatively charged phosphatidylserine lipid is mostly found at the inner leaflet of the plasma membrane,[15] and each membrane of the endocytic pathway but also the trans-Golgi network membrane and the plasma membrane are characterized by specific phosphoinositide content.[16,17] The plasma membrane, which contains saturated cylinder-shaped lipid species and high cholesterol levels, is characterized by tight lipid packing. On the other hand, the endoplasmic reticulum (ER) that exhibits high levels of unsaturated cone-shaped lipids and low levels of cholesterol is characterized by loose lipid packing.[12] Two distinct membrane territories have therefore been described: the late secretory pathway and the endocytic pathway (plasma membrane, endosomal membranes and trans-Golgi network) characterized by tight lipid packing and a highly charged cytosolic leaflet, and the early secretory pathway (ER and cis-Golgi) characterized by loose lipid packing and a weakly charged cytosolic leaflet. Of note, these varying lipid compositions are also relevant in the context of membrane order. The plasma membrane, which is enriched in saturated lipids and cholesterol, was shown to exist in both liquid-disordered (Ld) and liquid-ordered (Lo) states (so-called raft phase), while intracellular membranes composed of unsaturated lipids and low cholesterol levels rather behave as Ld phases.[18,19]

Membrane curvature is also a key feature of intracellular membranes as most cellular organelles display regions of both low and high curvatures. For example, the ER is formed of a complex network of interconnected flat sheets and highly curved tubules,[20,21] and endosomes display globular (low curvature) and tubular regions.[22] External constraints applied, for instance, by the cytoskeleton, protein coats or insertion of amphipathic protein domains can force a lipid bilayer to bend[23–25] and induce positive membrane curvature (convex surface detectable by cytosolic proteins), which gives rise to large lipid packing defects.[26] Lipid packing defects as well as membrane charge were described to be essential parameters regulating the specific membrane binding of some peripheral proteins.[16,26–30]

In this work, we investigate the role of membrane physicochemical properties in the binding of RAB proteins using *in vitro* assays consisting of purified RAB proteins and giant unilamellar vesicles (GUVs) as model membranes of controlled lipid composition.[31]

2 | RESULTS AND DISCUSSION

Four RAB proteins that localize to distinct membranes in cells were chosen for our study: RAB1 and RAB6 which associate with pre-Golgi and Golgi/trans-Golgi network membranes, respectively, RAB5 which is present on early endosomes and RAB35 which mainly localizes to the plasma membrane[32] (see Supporting information).

2.1 | RAB6 specifically localizes to the Ld phase independently of its prenylation state

To test whether RAB proteins show specific recruitment to a given lipid phase, we investigated the recruitment of purified RAB proteins to GUVs exhibiting phase separation between Lo and Ld domains.[33] GUVs were formed using a lipid mixture consisting of brain sphingomyelin (BSM), cholesterol and 1,2-dioleoyl-sn-glycero-3-phosphocholine (DOPC) (3:1:3 molar ratio).[34] No binding of unprenylated RAB proteins was observed on these membranes (Figure S1) which is in good agreement with the commonly accepted view that RAB proteins are incorporated into biological membranes through their C-terminal geranylgeranyl groups.[35] Most RAB GTPases are diprenylated in the cell with the addition of two geranylgeranyl moieties on the 2 C-terminal cysteines.[36] The use of diprenylated proteins (Figure S2A) is technically challenging because of the high affinity of the GDP-bound RAB for the REP,[37] which prevents binding to GUV membranes (Figure S3A-(1)). Recruitment of diprenylated RAB6 to membranes exhibiting phase separation was however achieved through the addition of the RAB binding domain of LidA ($LidA_{201\text{-}583}$) and GGTase I. LidA, a RAB6 supereffector from *Legionella pneumophila*, outcompetes the REP, while GGTase I shields the prenyl group from the solvent (detailed in Figure S3A). Under these conditions, diprenylated RAB6 was found to clearly segregate to the Ld phase (Figure S3A-(5)). Monoprenylated GDP-bound RAB6 (Figure S2B) also specifically binds to Ld membranes in the presence (Figure S3B) and also in the absence (Figure 1A) of these additional protein factors. These results demonstrate that $LidA_{201\text{-}583}$ and GGTase I do not influence protein membrane binding specificity and that both mono- and diprenylated RAB proteins preferentially bind to Ld membranes. To confirm these results, experiments were performed with GUVs composed of pure Ld phase (DOPC and cholesterol in a 1:1 molar ratio) or with GUVs composed of pure Lo phase (BSM and cholesterol in a 1:1 molar ratio).[34] GDP-bound RAB6, independently of its mono- or diprenylation status, was only recruited to Ld GUVs but not to Lo GUVs (Figures S3 and 1B). Thus, RAB6 displays similar membrane binding preferences toward Ld domains independently of its mono- or diprenylation status.

Although membrane binding specificity seemed to be unchanged, the kinetics of membrane dissociation were previously described to differ drastically between proteins harboring one or two lipid groups. *in vitro* studies using synthetic vesicles have indeed suggested that proteins that possess two geranylgeranyl modifications have a half-life of several hours[38] whereas monoprenylated proteins usually exhibit a half-life of 1 s or less.[39] In the same direction, more recent *in vitro* studies demonstrated that nonphysiological addition of a second farnesyl group to N-RAS proteins leads to reduced membrane dissociation rate.[40]

To investigate the kinetics of diffusion and association with membranes of mono- and diprenylated RAB proteins, we have performed fluorescence recovery after photobleaching experiments of GDP-bound RAB6 in complex with $LidA_{201\text{-}583}$ on DOPC-containing GUV membranes. RAB6 recovery by lateral diffusion was assessed by bleaching a small circular region of the GUV on the membrane close to the coverslip. Recovery curves yielded diffusion coefficients $D = 1.2 \pm 0.5$ $\mu m^2/s$ and $D = 1.3 \pm 0.2$ $\mu m^2/s$ for mono- and

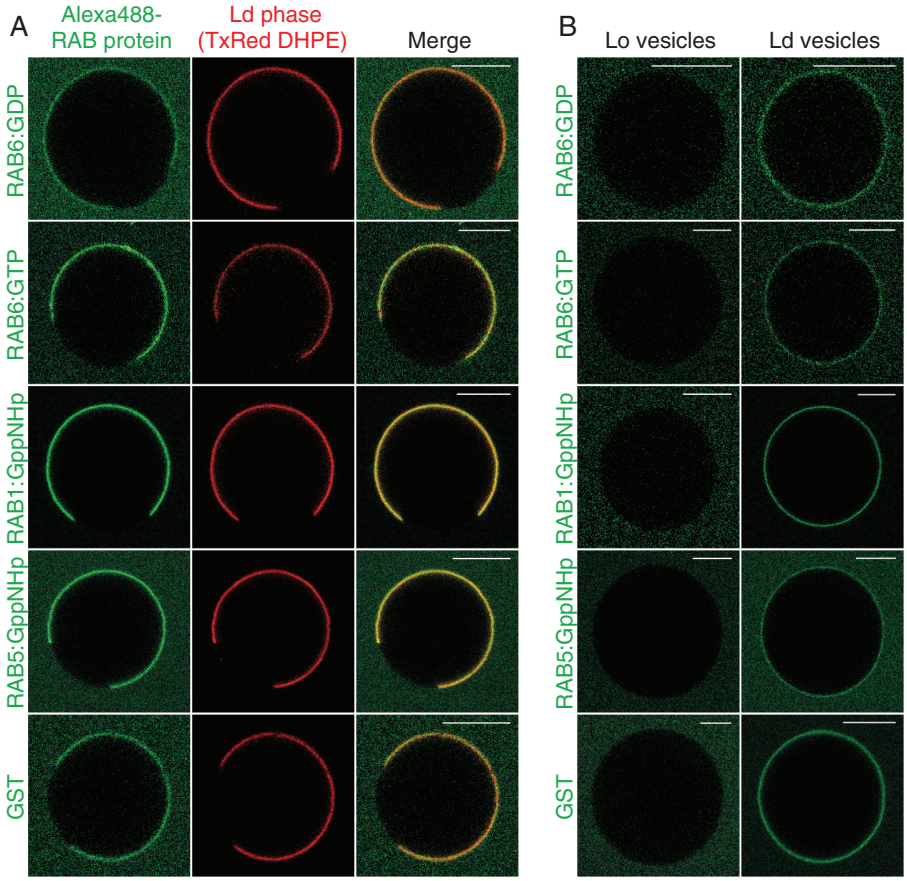

FIGURE 1 Monoprenylated proteins specifically bind to liquid-disordered domains independently of their activation/inactivation status. Prenylated proteins (RAB1, RAB5, RAB6 and GST) were labeled with Alexa488 fluorophore and monoprenylated. All images show GTP- or GppNHp-bound RAB proteins except for RAB6 which was also GDP-bound. GUVs were incubated with 2 μM protein. A, GUV phase separation was achieved using a 3:1:3 (molar ratios) BSM:cholesterol:DOPC lipid mixture. The Ld phase is marked with 0.1% (mol/mol) TexasRed-DHPE lipids whereas the Lo phase composed of saturated lipids is unlabeled. All tested proteins localize specifically to the Ld phase as shown by the merge images. B, Lo and Ld GUVs were, respectively, composed of 1:1 (molar ratios) BSM:cholesterol and DOPC:cholesterol. Prenylated proteins were recruited to Ld vesicles. but not to Lo vesicles (scale bar: 10 μm)

diprenylated RAB6, respectively, comparable to the diffusion coefficient of a TexasRed-labeled 1,2-dihexadecanoyl-sn-glycero-3-phosphoethanolamine (DHPE) lipid under the same conditions (D = 1.2 ± 0.3 μm^2/s) (Figure S4A). RAB6 recovery from the bulk was assessed by bleaching the full GUV and yielded recovery half-lives †$_{1/2}$ = 62 ± 18 seconds and †$_{1/2}$ = 414 ± 205 seconds for mono- and diprenylated RAB6, respectively (Figure S4B). These results indicate that monoprenylated RAB6 exhibits a faster recovery rate, which is in good agreement with previously published data.[38,39]

Although the recovery dynamics of mono- and diprenylated RAB6 were found to diverge, we have demonstrated that both were preferentially recruited to the same disordered membrane domains. This suggests that membrane binding kinetics have no influence on membrane binding preferences, making it possible to use monoprenylated RABs for this study.

In our experimental *in vitro* approach, activation (via nucleotide exchange) of diprenylated RABs leads to the dissociation of the REP–RAB complex and to the subsequent exposure of the hydrophobic prenyl groups to the solvent, thereby causing protein precipitation. In order to overcome this issue, diprenylated RABs can be activated in the presence of membranes which allows the stabilization of the prenyl groups, but consequently prevents any measurement of the amount of active GTP-bound RABs in our system. RAB proteins are however known to localize to the cytosol in their GDP-bound inactivated form and to get activated (GTP-bound) by GEFs upon membrane incorporation.[41] As membrane-bound RAB proteins are therefore mostly active, we decided for our study to investigate the binding of RAB proteins in their GTP-bound form. Because the efficiency of nucleotide exchange to GTP could not be measured when using diprenylated RAB proteins, this approach was only feasible using monoprenylated RAB proteins (Figure S2B). Therefore, we decided to focus our study on monoprenylated RAB proteins.

Some RAB proteins can undergo additional C-terminal modifications following geranylgeranylation, such as proteolysis and/or carboxyl methylation, depending on their prenylation motif.[42,43] RAB carboxyl methylation, which consists in the addition of a carboxyl group to the exposed prenylated cysteine, was shown to enhance the hydrophobicity of the C-terminus and subsequently to increase membrane affinity.[43] However, because the absence of methylation was shown to only affect the cycle of RAB membrane/cytosol partitioning, but not their specific membrane localization,[43] we did not investigate the potential effects of RAB carboxyl methylation in our *in vitro* experiments.

2.2 | RAB proteins specifically localize to the Ld phase through their geranylgeranyl group

Monoprenylated GTP-bound RAB6 was, like its GDP-bound counterpart, only recruited to Ld domains on GUVs displaying phase separation (Figure 1A) and recruitment was only observed on Ld vesicles but not on Lo vesicles (Figure 1B), indicating that the binding specificity of RAB6 is also independent of its activation state. Similarly to RAB6, monoprenylated and activated RAB1 and RAB5 segregated specifically to Ld domains on GUVs displaying phase separation (Figure 1A) and recruitment was only observed on Ld vesicles but not on Lo vesicles (Figure 1B).

We next investigated whether the prenyl group plays a direct role in the specific recruitment of RAB proteins to the Ld phase. For that purpose, we looked at the recruitment of glutathione S-transferase (GST) to which a CAAX prenylation motif (CVIL) was added at its C-terminus. The purified and fluorescently labeled protein was enzymatically monoprenylated using the same protocol that for the RAB proteins. As shown in Figure 1, monoprenylated GST also specifically segregated to Ld domains. On the other hand, no recruitment of unprenylated GST could either be detected on Lo or Ld domains (Figure S1), confirming that the prenyl group is required and sufficient for GST membrane insertion.

Altogether, the above results suggest that the recruitment of RAB proteins to Ld membranes is mediated by the geranylgeranyl moiety. Because of its bulky C20 isoprenoid highly unsaturated chain structure, the geranylgeranyl moiety (Figure S2C) might only be able to incorporate itself into Ld membranes. In agreement with this, previous studies have demonstrated that lipidated peptides containing isoprenyl groups or unsaturated acyl chains preferentially insert themselves into Ld membranes and show negligible affinity toward Lo membranes.[44] This preference for disordered domains was also shown for RAS proteins containing a C-terminal unsaturated C15 isoprenoid farnesyl group.[28,45] In contrast, peptides incorporating saturated acyl chains such as palmitoyl were found to be significantly recruited to Lo domains.[44] Similarly, the addition of a saturated C16 palmitoyl group to transmembrane proteins was shown to mediate their dynamic targeting to raft-like Lo phases.[46] Thus, a likely hypothesis is that the isoprenoid unsaturated structure of prenyl groups favors their insertion into Ld membranes.

2.3 | RAB35 membrane recruitment is driven by both the charged hypervariable region and the prenyl group

The great majority of RAB GTPases, including the previously tested RAB1, RAB5 and RAB6, are found associated with intracellular membranes.[32] RAB35, on the other hand, was shown to localize to intracellular endocytic compartments and also to the plasma membrane.[47] Thus, we wondered whether RAB35 membrane binding was governed by a similar mechanism. We first tested the recruitment of monoprenylated RAB35 to Lo and Ld GUVs. Unexpectedly, RAB35 was not recruited to either of these membranes (Figure 2A), indicating that the prenyl group is not sufficient to drive RAB35 membrane insertion.

Endosomal and plasma membranes are known to be negatively charged because of the large amount of phosphoinositides and phosphatidylserine,[11] anionic lipids known to play major roles in signaling processes and membrane dynamics.[16,48] RAB35 contains stretches of positively charged residues at its C-terminal region, the last 20 amino acid region being the most charged as compared with that of the other RABs (Table S1). *In cellulo* studies have shown that this polybasic region is essential for targeting RAB35 to the plasma membrane,[8] indicating that RAB35 localization depends on electrostatic interactions between the negative charge of the inner leaflet of the plasma membrane and the positive charges of the RAB35 C-terminal region. To address the role of electrostatic interactions, we monitored the recruitment of RAB35 to negatively charged GUVs containing 30 mol% 1-palmitoyl-2-oleoyl-*sn*-glycero-3-phospho-L-serine (POPS). RAB35 was efficiently recruited to POPS-containing vesicles, while no detectable interaction occurred when POPS was replaced by neutral 1-palmitoyl-2-oleoyl-*sn*-glycero-3-phosphocholine (POPC) (Figure 2A). These results demonstrate that RAB35 membrane recruitment is mediated by electrostatic interactions. We then investigated whether the prenyl group is required for RAB35 membrane binding to negatively charged POPS-containing vesicles. No binding of unprenylated RAB35 to charged vesicles was observed (Figure 2A), indicating that both the electrostatic interactions and the prenyl group are necessary for RAB35 recruitment.

In order to assess whether, as for the previously tested RABs, the prenyl group might also mediate specific membrane domain targeting, we monitored the recruitment of RAB35 to anionic Lo and Ld GUVs by replacing cholesterol with negatively charged sulfate cholesterol (see Supporting information). RAB35 membrane binding was now observed not only on Ld vesicles but also on Lo vesicles (Figure 2B). These results in combination with the absence of RAB35 recruitment to neutral Lo and Ld vesicles (Figure 2A) confirm that RAB35 membrane incorporation requires negatively charged lipids, and clearly demonstrate that in some cases the prenyl group is able to interact with Lo membranes. Additionally, we quantified the area density of prenylated RAB35 (Φ_v) using Equation (1) and observed a 3-fold increase in recruitment to Ld vesicles as compared with Lo vesicles (Figure 2B). This is consistent with the previous observations that prenylated proteins preferentially bind to Ld domains. Taken together, our results suggest that the membrane recruitment of C-terminally charged and prenylated RAB proteins is primarily dependent on the presence of anionic lipids. This specificity for negatively charged membranes gives the ability to RAB35 to overcome the exclusive binding of the prenyl group to Ld domains. This charge dependency is crucial for RAB35 interaction with negatively charged endosomal and plasma membranes. Interestingly, when comparing the charge of the last 20 amino acids of all human RAB proteins, we found that RAB23 and RAB35 display the highest positive charge (Table S1). RAB23 has also been shown to localize to the plasma membrane[49] suggesting that its specific recruitment to the plasma membrane might also be mediated by electrostatic interactions. Pointing in the same direction as our results, pioneer studies of McLaughlin et al. demonstrated that myristoylated alanine-rich C kinase substrate interacts with the negatively charged plasma membrane through a myristoyl-electrostatic switch involving the N-myristoyl group and a positively charged protein domain.[50,51] Additionally, more recent studies showed that the recruitment of proteins of the RAS family (K-RAS4B and RND3) to the plasma membrane can be modulated by electrostatic interactions between the positively charged C-terminus and anionic phospholipid headgroups.[52,53]

2.4 | RAB proteins can sense membrane curvature through their prenyl group

Most RAB proteins, for instance RAB1 or RAB6, are present on transport vesicles which typically have a diameter of 40-60 nm[54,55] and can thus be regarded as curved membranes. Therefore, we investigated

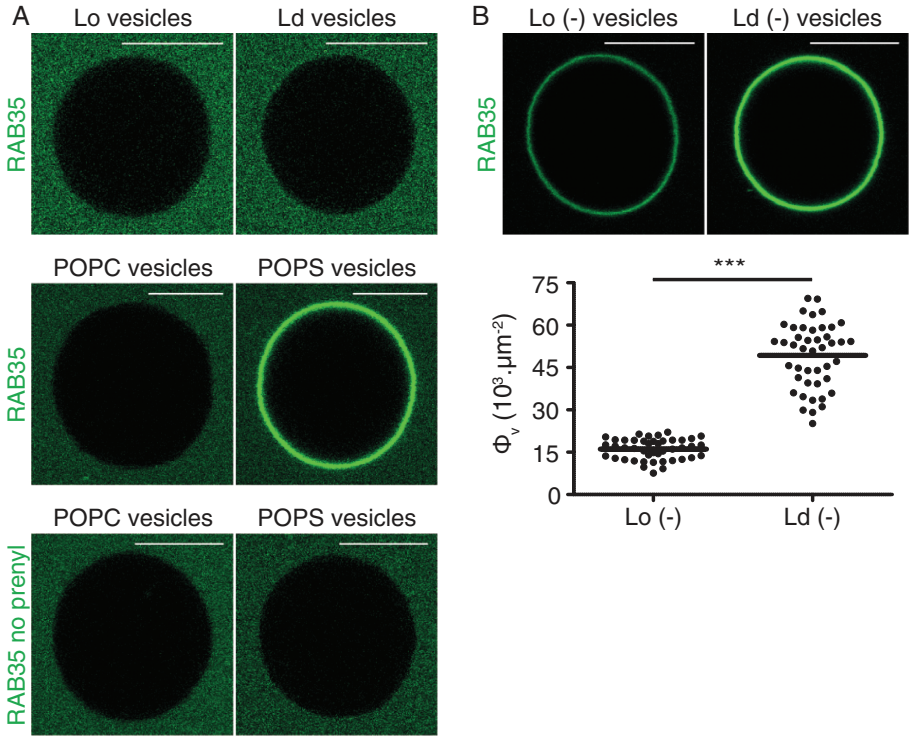

FIGURE 2 RAB35 membrane binding is both charge and prenyl group dependent. GUVs were incubated with 2 µM GFP-tagged RAB35. A, Neutral Lo and Ld vesicles were formed using 1:1 (molar ratios) of BSM:cholesterol and DOPC:cholesterol, respectively. Negatively charged POPS-containing vesicles were formed using a 30% POPS:30% cholesterol:40% EggPC (mol/mol) mix while neutral POPC-containing vesicles were formed by replacing POPS with POPC. Monoprenylated RAB35 was only recruited to negatively charged POPS-containing GUVs but not to neutral vesicles. Unprenylated RAB35 was not recruited to negatively charged POPS-containing vesicles. B, Negatively charged Lo and Ld vesicles were formed by replacing cholesterol with cholesterol sulfate. Monoprenylated RAB35 was recruited to both negatively charged Lo and Ld vesicles. Quantifications of GFP-RAB35 protein densities (Φ_v) show a 3-fold increase in RAB35 recruitment to disordered membranes. (scale bar: 10 µm; *** = *t*-test, *P*-value < 0.0001)

the influence of membrane curvature on RAB membrane recruitment. As a model, we used an optical tweezer setup to pull membrane tubes from L-α-phosphatidylcholine (Egg, Chicken) (EggPC) GUVs (with additional 0.1 mol% of TexasRed-DHPE lipids) (Figure S5A).[56,57] RAB protein relative enrichment (or sorting) between the highly curved tube and the flat GUV membrane was imaged by confocal microscopy. Tuning membrane tension through micropipette aspiration of the GUV allows us to modulate the tube radius and to measure protein sorting for increasing curvature (up to 1/15 nm^{-1}). Biological membranes are two-dimensional surfaces with two principal curvatures $C_1 = 1/R_1$ and $C_2 = 1/R_2$ (with R_1 and R_2 referred to as the principal radii of curvature) along two perpendicular directions.[58] The total curvature of the membrane is $C = C_1 + C_2$. In the case of a spherical vesicle of radius R, the membrane deforms equally in both directions leading to $C_1 = C_2 = 1/R$ and a total curvature $C_v = 2/R$. In the case of a cylindrical tube of radius R, which is curved only in one direction and flat in the other, $C_1 > 0$ and $C_2 = 0$ yielding a total curvature $C_t = 1/R$.[58] A 15 nm radius tube will thus have the same curvature as a 30 nm radius intracellular transport vesicle,[55] indicating that the typical curvatures in our experiments are biologically relevant.

Curvature sensing was assessed by calculating the sorting ratio (S) defined as the protein/lipid signal ratio on the tube divided by that observed on the GUV (Equation (2) and Figure S5B).[56,57] When the tube radius was decreased (ie, the curvature was increased), a clear enrichment of the proteins was detected in the tube region (Figure 3A). Sorting was different among the studied RAB proteins, with a ratio increasing up to 5.5, 3 and 2.5 times at a 15 nm tube radius for RAB5, RAB6 and RAB1, respectively.

Because curvature sensing depends on the protein area density (Φ_v),[57] sorting values cannot be directly compared among RAB proteins. The protein density is coupled to membrane curvature through a protein curvature coupling coefficient (also called protein spontaneous curvature, C_p).[57] To quantitatively compare the sorting of RAB proteins with that of other proteins, we used the theoretical model previously developed by Sorre et al.[57] and the resulting equation $S = 1 + 1/(R_t C_p \varphi_v)$, where S is the sorting ratio, R_t is the tube radius, C_p is the effective spontaneous curvature of the protein and φ_v is the protein area fraction which is related to Φ_v by $\Phi_v = \rho\varphi_v$ (ρ is the inverse of the area per protein). The intrinsic curvature radius of the protein C_p^{-1} can be determined by plotting $(S - 1)\ \varphi_v$ as a function of curvature ($1/R_t$) and taking the resulting slope of the linear fit (Figure 3B). Φ_v was assessed using Equation (1) and ρ was estimated by assuming that RAB proteins are spherical proteins of around 25 kDa with a corresponding average radius of 2 nm (ρ = 1/12.6 nm^{-2}).[59] C_p^{-1} values were, respectively, 2.1 ± 0.6, 2.6 ± 0.7 and 1.5 ± 0.5 nm for RAB1, RAB5 and RAB6. RAB proteins interact with membranes through the hydrophobic insertion of their prenyl group into the bilayer while a few amino acid residues close to the prenylation site will be in proximity to the lipid headgroups. Thus, the geometry of the inserted domain may be comparable to that of the Epsin N-Terminal Homology (ENTH) domain which senses membrane curvature through an amphipathic helix, but also to that of lipids with inverted conical shapes, such as lysophosphatidic acids (LPAs). The first was described to exhibit a spontaneous curvature radius of 1.6 nm,[60] while the latter was shown to generate local positive curvature and to display a spontaneous curvature radius of 2 nm.[58] The spontaneous curvature values of ENTH domains and LPAs are therefore both very similar to those we obtained for RAB proteins. Our values are also very similar to that of Amphiphysin (1.9 ± 0.4 nm) which was calculated using the same low-density

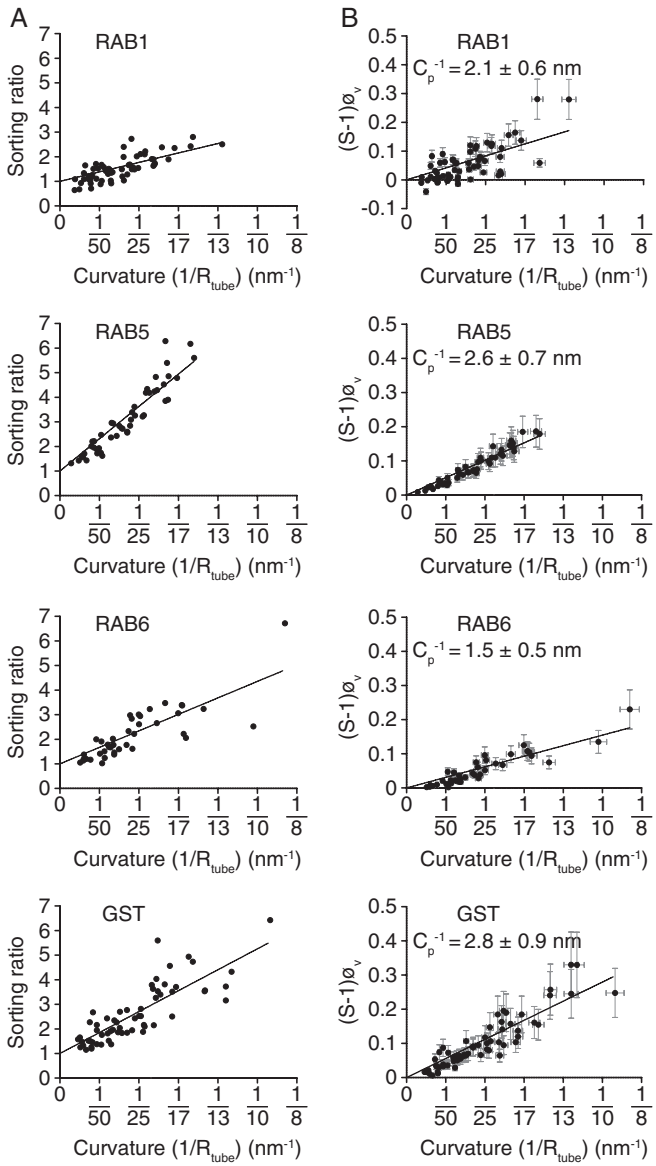

FIGURE 3 Prenylated proteins can sense membrane curvature. A highly curved membrane tube was pulled with optical tweezers from an EggPC GUV containing the fluorescent lipid marker TexasRed-DHPE (red) in the presence of 100-300 nM Alexa488 labeled monoprenylated proteins (RAB1, RAB5, RAB6 and GST). A, The plots show the protein sorting ratios (calculated using Equation (2)) as a function of tube curvature ($1/R_{tube}$) and each dot represents one sorting measurement at a given tube radius. Data were obtained from 10 (RAB1 and GST) or 7 (RAB5 and RAB6) independent experiments. Each plot was fitted with a linear regression (black line). For all prenylated proteins, sorting increases when the curvature is increased (ie, when the tube radius is decreased). B, The protein effective spontaneous curvatures were calculated using the theoretical model from Sorre et al.[57] in which the sorting ratio S is given by $S = 1 + 1/(R_t C_p \varphi_v)$, where R_t is the tube radius, C_p is the effective spontaneous curvature of the protein and φ_v is the protein area fraction (related to the protein density Φ_v by $\Phi_v = \rho\varphi_v$, ρ = inverse of the area per protein = 1/12.6 nm^{-2}). $(S - 1)\varphi_v$ is thus predicted to scale linearly with the tube curvature ($1/R_t$) with a slope C_p^{-1}. By using the same sorting ratio values as obtained in (A) and measuring the protein density on the GUV, we plotted $(S - 1)\ \varphi_v$ as a function of curvature ($1/R_t$). The spontaneous curvature radius value was determined by fitting the plot with a linear regression and extracting the value of the slope. Error bars correspond to the experimental errors of the measurements

regime model (when no apparent GUV membrane deformation could be observed).[57] However, Amphiphysin was described to sense curvature not only through the insertion of an amphipathic helix but also through its curved Bin/Amphiphysin/Rvs domain[61,62] which suggests that RAB and Amphiphysin C_p^{-1} values might not be directly comparable. Even though RAB proteins were observed to preferentially sort into the highly curved tube, RAB proteins also bind to flat GUV membranes indicating that RAB membrane binding is not primarily dependent on curvature. In contrast to this, amphipathic lipid packing sensor (ALPS) motifs were described to interact specifically with highly curved membranes (tube radii lower than 35 nm).[56] RAB sensitivity to membrane curvature is therefore weak compared with that of ALPS motif-containing proteins. Our finding that RAB proteins bind to both flat and curved membranes, with a slight preference for the latter, is consistent with the binding of RAB proteins to both flat organelle membranes and curved transport vesicles in cells.

We next investigated the contribution of the prenyl group to the sensitivity of RAB proteins for curved membranes using monoprenylated GST. As shown in Figure 3A, a clear enrichment of monoprenylated GST in membrane tubes pulled from GUVs was observed (4-fold increase on tubes of 15 nm radius). The spontaneous curvature radius of monoprenylated GST was measured using the same model as above. We found $C_p^{-1} = 2.8 \pm 0.9$ nm, which is very similar to the values obtained for RAB proteins (Figure 3B). This suggests that RAB curvature sensing is independent of the tertiary structure of the protein but, similarly to their preference for Ld membranes, depends on the geranylgeranyl moiety.

2.5 | Prenylated proteins show preferences for lipid packing defects

The Ld phase is characterized by the assembly of unsaturated lipids which are known to promote lipid packing defects.[12] Membrane curvature was also shown to lead to the appearance of defects in the arrangement of lipids.[12] To explain the preferential binding of RAB proteins to Ld membranes and their sensitivity to curvature, we hypothesized that RAB membrane recruitment is dependent on the presence of lipid packing defects in the bilayer.

To test this hypothesis, we performed recruitment experiments with GUVs containing 15 mol% 1-2-dioleoyl-*sn*-glycerol (DOG), a conical-shaped lipid that was shown to induce the formation of packing defects similar to those found on positively curved membranes.[63] Control GUVs containing lower amounts of lipid packing defects were composed of 15 mol% DOPC cylindrical lipids (see Supporting information). The membrane recruitment of all monoprenylated proteins was significantly increased in the presence of DOG (Figure 4), that is, in the presence of higher amounts of lipid packing defects.

Unlike DOG, polyunsaturated fatty acids (PUFAs), such as 1-stearoyl-2-docosahexaenoyl-sn-glycero-3-phosphoethanolamine (PUFA PE), were shown to decrease the amount of lipid packing defects, especially in curved membranes.[64] We measured RAB and GST binding on GUVs composed of 30 mol% PUFA PE and used as a control GUVs containing higher amounts of packing defects and composed of 30 mol% 1-palmitoyl-2-oleoyl-sn-glycero-3-phosphoethanolamine

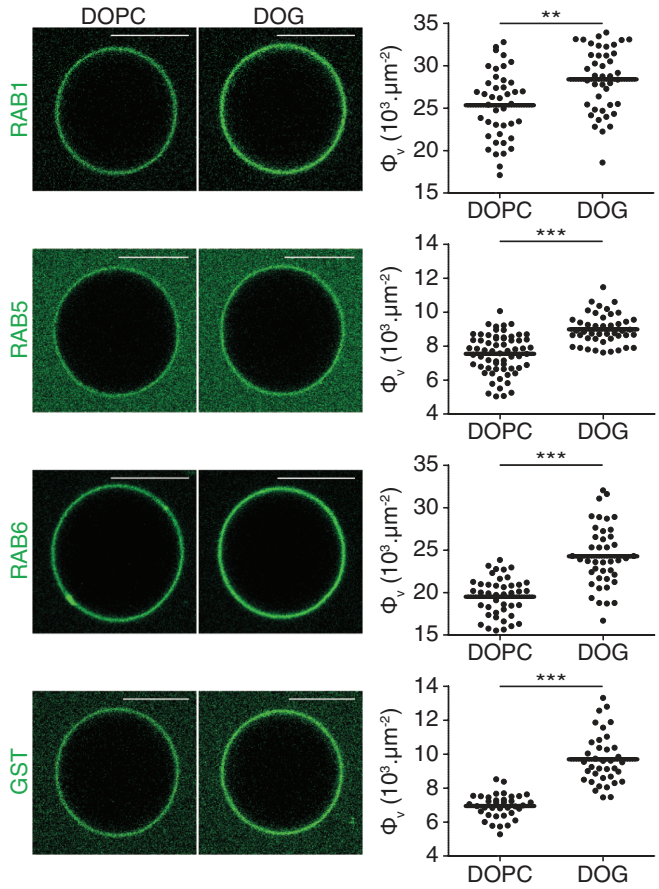

FIGURE 4 Increasing amounts of lipid packing defects enhance RAB membrane binding. RAB1, RAB5, RAB6 and GST were labeled using Alexa488, monoprenylated and incubated with GUVs at 2 µM final concentration. DOG-containing GUVs with a high density of lipid packing defects were formed using an 85% EggPC:15% DOG (mol/mol) mix. In control GUVs, DOPC replaced DOG. The right panel shows the quantification of protein density on the membrane (Φ_v) in both DOPC and DOG containing vesicles. We observed a significant increase in protein recruitment on GUVs with higher levels of lipid packing defects. (scale bar: 10 µm; *** = *t*-test, *P*-value < 0.0001; ** = *t*-test, *P*-value = 0.0006)

(POPE) (see Supporting information). We found that the membrane recruitment of geranylgeranylated proteins significantly decreases in the presence of PUFA PE (Figure 5), that is, when the amount of packing defects is decreased.

Altogether, the above results suggest that lipid packing defects are drivers of RAB membrane recruitment and that this lipid packing defect sensing is mediated by the C-terminal prenyl group.

3 | CONCLUSION

It has been known for a long time that prenyl groups act as nonspecific membrane anchors but our results, together with recently published data,[28,29] highlight a role for prenyl groups (farnesyl and geranylgeranyl) in specific membrane domain targeting. Similarly to what we found with geranylgeranylated RAB proteins, farnesylated N-RAS preferentially binds to Ld domains on flat membranes and its differential membrane recruitment was shown to rely on the presence of lipid packing defects induced by curvature and specific lipid geometrical shapes.[28,29] A likely explanation is that prenyl groups are largely unsaturated and have a kinked structure allowing them to get preferentially inserted into membranes containing packing defects such as Ld or curved membranes.

This lipid-driven membrane binding mechanism sheds new light on how RAB GTPases could bind to membranes. Intracellular membranes are mainly composed of Ld phases,[18] and many RAB proteins associate with highly curved transport vesicles.[54,55] Our hypothesis is that the addition of one or two geranylgeranyl moieties on all RAB proteins serves as a core mechanism to bind them to specific membrane domains displaying lipid packing defects, the specificity for a given compartment (ER, Golgi and endosomes) relying then on other mechanisms such as the presence of specific GEFs.[3]

An interesting variation to this theme is given by RAB35 which has a positively charged C-terminus and is mainly found at steady state associated with the plasma membrane and the endocytic compartments.[47] We showed that RAB35 membrane recruitment is primarily dependent on the presence of negatively charged lipids which are also predominantly found on endosomal and plasma membranes.[11] Even though lipid packing defects enhance RAB35 membrane affinity, they are not essential for membrane binding.

In conclusion, our work illustrates that the physicochemical properties of membranes, such as charge distribution and lipid packing defects, could be prime determinants of the localization of RAB proteins to cellular membranes.

4 | MATERIAL AND METHODS

4.1 | *In vitro* monoprenylation and diprenylation

The prenylation reaction consists in the addition of one or two C20 geranylgeranyl moieties (geranylgeranyl pyrophosphate, GGpp; Sigma) at the C-terminal extremity of the proteins. Prenylation was achieved either through monoprenylation (addition of one geranylgeranyl group) using purified geranylgeranyl transferase type I (GGTase I) (Figure S2B) or diprenylation (addition of two geranylgeranyl groups) using the native prenylation machinery consisting of purified RAB geranylgeranyl transferase (RABGGTase or GGTase II) and REP (Figure S2A).

Monoprenylation reactions were performed at 25°C for 1.5 hours with a molar ratio of 0.5:1:5 GGTase I, RAB and GGpp. Molar ratios for the diprenylation reaction were 1:5:0.5:0.75 RABGGTase:GGpp:RAB:REP and the reaction was performed at 25°C for 4 hours. To control efficient protein prenylation, nitrobenzoxadiazole (NBD)-farnesyl pyrophosphate (Jena Bioscience), a C15 fluorescent analog of geranylgeranyl pyrophosphate, was used as described previously.[65]

4.2 | Giant unilamellar vesicles

GUVs were grown on indium tin oxide (ITO)-coated glass slides using the electroformation technique.[66] Fifteen microliters of a 0.5 mg/mL lipid mix was dried on ITO-coated slides for a few minutes at 50°C and subsequently under vacuum for at least

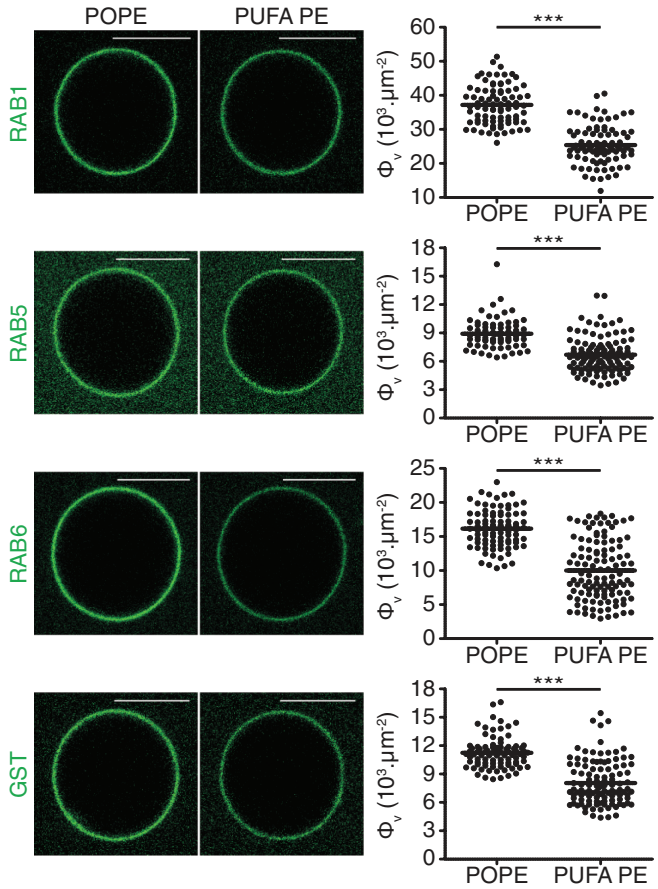

FIGURE 5 Decreasing amounts of lipid packing defects reduce RAB membrane binding. RAB1, RAB5, RAB6 and GST were labeled using Alexa488, monoprenylated and incubated with GUVs at 2 μM final concentration. PUFA PE containing GUVs with a low density of lipid packing defects were formed using a 55% EggPC:15% DOG:30% PUFA PE (mol/mol) mix. In control GUVs POPE replaced PUFA PE. The right panel represents the quantification of protein density on the membrane (Φ_v) in both POPE and PUFA PE containing vesicles. We observed a significant decrease in protein recruitment on GUVs with lower levels of lipid packing defects. (scale bar: 10 μm; *** = *t*-test, *P*-value < 0.0001)

2 hours. The dried lipid film was then rehydrated in a sucrose solution (osmolarity between 100 and 430 mOsm depending on the osmolarity of the protein buffer used for the experiments) and GUVs were grown for 3 hours under a sinusoïdal voltage (1.1 V, 10 Hz). GUV growth was most of the time performed at room temperature except in the case of phase separation (see Supporting information) where it was performed at 50°C.

4.3 | Membrane tube pulling by optical tweezers

A highly curved membrane tube was pulled out from an EggPC containing GUV, aspirated in a micropipette to control its membrane tension, using 3.2 μm diameter beads trapped in an optical tweezer (Figure S5A) as previously described.[56] The membrane tension was increased in a stepwise fashion to decrease the tube radius and hence increase membrane curvature.[56] The reaction buffer used was the one specific of the studied protein and was supplemented with 0.1 mg/mL β-Casein to prevent adhesion of the GUV to the glass. Membrane binding was studied using 100-300 nM final concentration of protein.

4.4 | Measurement of protein density on the membrane

Protein density was assessed as previously described.[57] Briefly, fluorescence was calibrated using GUVs made of EggPC lipids and BodipyFL-C5-1-hexadecanoyl-sn-glycero-3-phosphocholine (HPC), a green fluorescent lipid, at various concentrations. The HPC area density on the GUV (Φ_v^{HPC}) can be calculated by assuming that the average area occupied by a single phosphatidylcholine (PC) molecule is 0.7 nm^2.[67] The fluorescent intensity of this lipid on the GUV membrane was measured (I_v^{HPC} at a given confocal photomultiplier tube detector gain) for each area density. A linear fit of the fluorescence vs area density plot gave the conversion constant (A_{gain}) ($\Phi_v^{HPC} = A_{gain} \times I_v^{HPC}$). Proteins were labeled with the Alexa488 fluorophore and lipids with BodipyFL-C5-HPC, two fluorophore exhibiting different spectral properties. Thus, we measured the correction factor $F = I_{bulk}^{A488} / I_{bulk}^{HPC}$, that is, the ratio of fluorescence intensities of Alexa488 and HPC, respectively, at a given concentration in solution. Both fluorescent signals in bulk scaled linearly with their concentration and *F* is defined as the ratio between the slopes of the Alexa488 linear fit and that of HPC. The protein labeling efficiency was taken into account by calculating the degree of labeling (n^*) of the protein using Equation S1. Protein density on the GUV membrane (Φ_v^{prot}) was thus given by

$$\Phi_v^{prot} = \frac{A_{gain}}{F\,x\,n^*} \times I_v^{prot}\,(\text{gain}) \quad (1)$$

4.5 | Measurement of sorting ratio

In order to quantify protein sorting to the tube, the fluorescence intensity of the Alexa488 labeled protein ($I_{protein}$) was normalized by the intensity of the fluorescent lipid (TexasRed-DHPE, I_{lipid}) at each tension step increase. The sorting ratio *S* corresponds to the ratio between the normalized protein intensity on the tube and the same normalized intensity on the GUV (Figure S5B):

$$S = \frac{\left(I_{protein}/I_{lipid}\right)_{tube}}{\left(I_{protein}/I_{lipid}\right)_{vesicle}} \quad (2)$$

ACKNOWLEDGMENTS

We thank Roger Goody for providing the plasmids to express the prenylation machinery. Ahmed El Marjou is acknowledged for the purification of the REP protein. We thank Aymelt Itzen for critical reading of the manuscript. We thank Bruno Antonny, Sandrine Etienne-Manneville and Jean-Claude Guillemot for stimulating discussions. We thank Ernesto Ambroggio, Maryam Alqabandi and Feng-Ching Tsai for their help with the fluorescence quantifications. We thank Mathieu Pinot for his technical assistance with the optical tweezer setup. This work was supported by an European Research

Council (ERC) advanced grant (project 339847 "MYODYN"). The Goud team is a member of Labex CelTisPhyBio (11-LBX-038). L.K.O. was supported by a Marie Curie Intra European Fellowship (PIEF-GA-2012-326649).

Conflict of interest

The authors declare no potential conflict of interests.

The Editorial Process File is available in the online version of this article.

ORCID

Lena K. Oesterlin http://orcid.org/0000-0003-3074-2921

REFERENCES

1. Alexandrov K, Horiuchi H, Steele-Mortimer O, Seabra MC, Zerial M. Rab escort protein-1 is a multifunctional protein that accompanies newly prenylated Rab proteins to their target membranes. *EMBO J*. 1994;13(22):5262-5273.
2. Alory C, Balch WE. Organization of the Rab-GDI/CHM superfamily: the functional basis for choroideremia disease. *Traffic*. 2001;2(8):532-543.
3. Blumer J, Rey J, Dehmelt L, et al. RabGEFs are a major determinant for specific Rab membrane targeting. *J Cell Biol*. 2013;200(3):287-300.
4. Hutt DM, Da-Silva LF, Chang LH, Prosser DC, Ngsee JK. PRA1 inhibits the extraction of membrane-bound Rab GTPase by GDI1. *J Biol Chem*. 2000;275(24):18511-18519.
5. Sivars U, Aivazian D, Pfeffer SR. Yip3 catalyses the dissociation of endosomal Rab–GDI complexes. *Nature*. 2003;425(6960):856-859.
6. Pereira-Leal JB, Seabra MC. The mammalian Rab family of small GTPases: definition of family and subfamily sequence motifs suggests a mechanism for functional specificity in the Ras superfamily. *J Mol Biol*. 2000;301(4):1077-1087.
7. Ali BR, Wasmeier C, Lamoreux L, Strom M, Seabra MC. Multiple regions contribute to membrane targeting of Rab GTPases. *J Cell Sci*. 2004;117(Pt 26):6401-6412.
8. Li F, Yi L, Zhao L, Itzen A, Goody RS, Wu YW. The role of the hypervariable C-terminal domain in Rab GTPases membrane targeting. *Proc Natl Acad Sci U S A*. 2014;111(7):2572-2577.
9. Singer SJ, Nicolson GL. The fluid mosaic model of the structure of cell membranes. *Science*. 1972;175(4023):720-731.
10. Engelman DM. Membranes are more mosaic than fluid. *Nature*. 2005;438(7068):578-580.
11. van Meer G, Voelker DR, Feigenson GW. Membrane lipids: where they are and how they behave. *Nat Rev Mol Cell Biol*. 2008;9(2):112-124.
12. Bigay J, Antonny B. Curvature, lipid packing, and electrostatics of membrane organelles: defining cellular territories in determining specificity. *Dev Cell*. 2012;23(5):886-895.
13. Holthuis JC, Menon AK. Lipid landscapes and pipelines in membrane homeostasis. *Nature*. 2014;510(7503):48-57.
14. Jackson CL, Walch L, Verbavatz JM. Lipids and their trafficking: an integral part of cellular organization. *Dev Cell*. 2016;39(2):139-153.
15. Yeung T, Gilbert GE, Shi J, Silvius J, Kapus A, Grinstein S. Membrane phosphatidylserine regulates surface charge and protein localization. *Science*. 2008;319(5860):210-213.
16. Di Paolo G, De Camilli P. Phosphoinositides in cell regulation and membrane dynamics. *Nature*. 2006;443(7112):651-657.
17. Jean S, Kiger AA. Coordination between RAB GTPase and phosphoinositide regulation and functions. *Nat Rev Mol Cell Biol*. 2012;13(7):463-470.
18. Niko Y, Didier P, Mely Y, Konishi G, Klymchenko AS. Bright and photostable push–pull pyrene dye visualizes lipid order variation between plasma and intracellular membranes. *Sci Rep*. 2016;6:18870.
19. Mazeres S, Fereidouni F, Joly E. Using spectral decomposition of the signals from laurdan-derived probes to evaluate the physical state of membranes in live cells. *F1000Research*. 2017;6:763.
20. Voeltz GK, Prinz WA. Sheets, ribbons and tubules—how organelles get their shape. *Nat Rev Mol Cell Biol*. 2007;8:258-264.
21. Shibata Y, Hu J, Kozlov MM, Rapoport TA. Mechanisms shaping the membranes of cellular organelles. *Annu Rev Cell Dev Biol*. 2009;25:329-354.
22. Sonnichsen B, De Renzis S, Nielsen E, Rietdorf J, Zerial M. Distinct membrane domains on endosomes in the recycling pathway visualized by multicolor imaging of Rab4, Rab5, and Rab11. *J Cell Biol*. 2000;149(4):901-914.
23. McMahon HT, Boucrot E. Membrane curvature at a glance. *J Cell Sci*. 2015;128(6):1065-1070.
24. Graham TR, Kozlov MM. Interplay of proteins and lipids in generating membrane curvature. *Curr Opin Cell Biol*. 2010;22(4):430-436.
25. Kozlov MM, Campelo F, Liska N, Chernomordik LV, Marrink SJ, McMahon HT. Mechanisms shaping cell membranes. *Curr Opin Cell Biol*. 2014;29:53-60.
26. Antonny B. Mechanisms of membrane curvature sensing. *Annu Rev Biochem*. 2011;80:101-123.
27. Cui H, Lyman E, Voth GA. Mechanism of membrane curvature sensing by amphipathic helix containing proteins. *Biophys J*. 2011;100(5):1271-1279.
28. Larsen JB, Jensen MB, Bhatia VK, et al. Membrane curvature enables N-Ras lipid anchor sorting to liquid-ordered membrane phases. *Nat Chem Biol*. 2015;11(3):192-194.
29. Larsen JB, Kennard C, Pedersen SL, et al. Membrane curvature and lipid composition synergize to regulate N-Ras anchor recruitment. *Biophys J*. 2017;113(6):1269-1279.
30. Heo WD, Inoue T, Park WS, et al. PI(3,4,5)P3 and PI(4,5)P2 lipids target proteins with polybasic clusters to the plasma membrane. *Science*. 2006;314(5804):1458-1461.
31. Walde P, Cosentino K, Engel H, Stano P. Giant vesicles: preparations and applications. *Chembiochem*. 2010;11(7):848-865.
32. Hutagalung AH, Novick PJ. Role of Rab GTPases in membrane traffic and cell physiology. *Physiol Rev*. 2011;91(1):119-149.
33. Baumgart T, Hess ST, Webb WW. Imaging coexisting fluid domains in biomembrane models coupling curvature and line tension. *Nature*. 2003;425(6960):821-824.
34. Roux A, Cuvelier D, Nassoy P, Prost J, Bassereau P, Goud B. Role of curvature and phase transition in lipid sorting and fission of membrane tubules. *EMBO J*. 2005;24(8):1537-1545.
35. Pechlivanis M, Kuhlmann J. Hydrophobic modifications of Ras proteins by isoprenoid groups and fatty acids—more than just membrane anchoring. *Biochim Biophys Acta*. 2006;1764(12):1914-1931.
36. Gomes AQ, Ali BR, Ramalho JS, et al. Membrane targeting of Rab GTPases is influenced by the prenylation motif. *Mol Biol Cell*. 2003;14(5):1882-1899.
37. Wu YW, Oesterlin LK, Tan KT, Waldmann H, Alexandrov K, Goody RS. Membrane targeting mechanism of Rab GTPases elucidated by semisynthetic protein probes. *Nat Chem Biol*. 2010;6(7):534-540.
38. Shahinian S, Silvius JR. Doubly-lipid-modified protein sequence motifs exhibit long-lived anchorage to lipid bilayer membranes. *Biochemistry*. 1995;34(11):3813-3822.
39. Schroeder H, Leventis R, Rex S, et al. S-acylation and plasma membrane targeting of the farnesylated carboxyl-terminal peptide of N-ras in mammalian fibroblasts. *Biochemistry*. 1997;36(42):13102-13109.
40. Gohlke A, Triola G, Waldmann H, Winter R. Influence of the lipid anchor motif of N-ras on the interaction with lipid membranes: a surface plasmon resonance study. *Biophys J*. 2010;98(10):2226-2235.
41. Stenmark H. Rab GTPases as coordinators of vesicle traffic. *Nat Rev Mol Cell Biol*. 2009;10(8):513-525.
42. Smeland TE, Seabra MC, Goldstein JL, Brown MS. Geranylgeranylated Rab proteins terminating in Cys-Ala-Cys, but not Cys-Cys, are carboxyl-methylated by bovine brain membranes in vitro. *Proc Natl Acad Sci U S A*. 1994;91(22):10712-10716.
43. Leung KF, Baron R, Ali BR, Magee AI, Seabra MC. Rab GTPases containing a CAAX motif are processed post-geranylgeranylation by proteolysis and methylation. *J Biol Chem*. 2007;282(2):1487-1497.

44. Wang TY, Leventis R, Silvius JR. Partitioning of lipidated peptide sequences into liquid-ordered lipid domains in model and biological membranes. *Biochemistry*. 2001;40(43):13031-13040.
45. Jang H, Abraham SJ, Chavan TS, et al. Mechanisms of membrane binding of small GTPase K-Ras4B farnesylated hypervariable region. *J Biol Chem*. 2015;290(15):9465-9477.
46. Levental I, Lingwood D, Grzybek M, Coskun U, Simons K. Palmitoylation regulates raft affinity for the majority of integral raft proteins. *Proc Natl Acad Sci U S A*. 2010;107(51):22050-22054.
47. Kouranti I, Sachse M, Arouche N, Goud B, Echard A. Rab35 regulates an endocytic recycling pathway essential for the terminal steps of cytokinesis. *Curr Biol*. 2006;16(17):1719-1725.
48. Raghupathy R, Anilkumar AA, Polley A, et al. Transbilayer lipid interactions mediate nanoclustering of lipid-anchored proteins. *Cell*. 2015;161(3):581-594.
49. Evans TM, Ferguson C, Wainwright BJ, Parton RG, Wicking C. Rab23, a negative regulator of hedgehog signaling, localizes to the plasma membrane and the endocytic pathway. *Traffic*. 2003;4(12):869-884.
50. Peitzsch RM, McLaughlin S. Binding of acylated peptides and fatty acids to phospholipid vesicles: pertinence to myristoylated proteins. *Biochemistry*. 1993;32(39):10436-10443.
51. McLaughlin S, Aderem A. The myristoyl-electrostatic switch: a modulator of reversible protein–membrane interactions. *Trends Biochem Sci*. 1995;20(7):272-276.
52. Gomez GA, Daniotti JL. Electrical properties of plasma membrane modulate subcellular distribution of K-Ras. *FEBS J*. 2007;274(9):2210-2228.
53. Madigan JP, Bodemann BO, Brady DC, et al. Regulation of Rnd3 localization and function by protein kinase C alpha-mediated phosphorylation. *Biochem J*. 2009;424(1):153-161.
54. McMahon HT, Boucrot E. Molecular mechanism and physiological functions of clathrin-mediated endocytosis. *Nat Rev Mol Cell Biol*. 2011;12(8):517-533.
55. Takamori S, Holt M, Stenius K, et al. Molecular anatomy of a trafficking organelle. *Cell*. 2006;127(4):831-846.
56. Ambroggio E, Sorre B, Bassereau P, Goud B, Manneville JB, Antonny B. ArfGAP1 generates an Arf1 gradient on continuous lipid membranes displaying flat and curved regions. *EMBO J*. 2010;29(2):292-303.
57. Sorre B, Callan-Jones A, Manzi J, et al. Nature of curvature coupling of amphiphysin with membranes depends on its bound density. *Proc Natl Acad Sci U S A*. 2012;109(1):173-178.
58. Zimmerberg J, Kozlov MM. How proteins produce cellular membrane curvature. *Nat Rev Mol Cell Biol*. 2006;7(1):9-19.
59. Erickson HP. Size and shape of protein molecules at the nanometer level determined by sedimentation, gel filtration, and electron microscopy. *Biol Proced Online*. 2009;11:32-51.
60. Capraro BR, Yoon Y, Cho W, Baumgart T. Curvature sensing by the epsin N-terminal homology domain measured on cylindrical lipid membrane tethers. *J Am Chem Soc*. 2010;132(4):1200-1201.
61. Peter BJ, Kent HM, Mills IG, et al. BAR domains as sensors of membrane curvature: the amphiphysin BAR structure. *Science*. 2004;303(5657):495-499.
62. Bhatia VK, Madsen KL, Bolinger PY, et al. Amphipathic motifs in BAR domains are essential for membrane curvature sensing. *EMBO J*. 2009;28(21):3303-3314.
63. Vamparys L, Gautier R, Vanni S, et al. Conical lipids in flat bilayers induce packing defects similar to that induced by positive curvature. *Biophys J*. 2013;104(3):585-593.
64. Pinot M, Vanni S, Pagnotta S, et al. Lipid cell biology. Polyunsaturated phospholipids facilitate membrane deformation and fission by endocytic proteins. *Science*. 2014;345(6197):693-697.
65. Dursina B, Reents R, Delon C, et al. Identification and specificity profiling of protein prenyltransferase inhibitors using new fluorescent phosphoisoprenoids. *J Am Chem Soc*. 2006;128(9):2822-2835.
66. Angelova M, Soléau S, Méléard P, Faucon JF, Bothorel P. Preparation of giant vesicles by external AC electric fields. Kinetics and applications. *Prog Colloid Polym Sci*. 1992;89:127-131.
67. Nagle JF, Tristram-Nagle S. Structure of lipid bilayers. *Biochim Biophys Acta*. 2000;1469(3):159-195.

SUPPORTING INFORMATION

Additional Supporting Information may be found online in the supporting information tab for this article.

How to cite this article: Kulakowski G, Bousquet H, Manneville J-B, Bassereau P, Goud B, Oesterlin LK. Lipid packing defects and membrane charge control RAB GTPase recruitment. *Traffic*. 2018;19:536–545. https://doi.org/10.1111/tra.12568